Supporting Information

Experimental and related aspects

Characterization:

The synthesized materials were characterized by different techniques. X-ray diffraction (XRD) data of all samples were collected by the X'Pert PRO PANanalytical equipment (Bragg-Brentano geometry with automatic divergence slits, position sensitive detector, continuous mode, room temperature, Cu-Kα radiation, Ni filter. The powder samples were dropped onto silicon wafer with grease, and measured at the same equipment (5-80°, at a step of 0.0197°, with accumulation time 200 s per step). The morphology and porous nature characterized through scanning electron microscopy (FESEM-FEI Nova-Nano SEM-600) and transmission electron microscope (JEOL JEM-3010 with accelerating voltage at 300 kV). The Raman spectra were recorded in backscattering arrangement, using 532 nm laser excitation using 6 mW laser power. Elemental analyses were carried out using a Thermo Scientific Flash 2000 CHN analyzer. X-ray photoelectron spectroscopy (XPS) was performed on a PHI 5000 Versa Probe II scanning XPS microprobe from Physical Electronics, using X-ray radiation from an Al source equipped with a monochromator. Spectra were collected and evaluated with the MultiPak (ULVAC-PHI, Inc.) software. All binding energies were referenced to the C1s peak at 284.8 eV. Adsorption studies of N_2 (77 K) of all samples were carried out using MICROMERITICS analyzer, outgassed at 423 K under high vacuum. The Raman spectrum of respective sample were collected through instrument, DXR Raman (Thermo, USA); laser wavelength: 633 nm, laser power on sample: 2mW, exposition time: 5s, 32 spectra were averaged at each spot to obtain one data point. UV-Vis diffuse reflectance spectra were recorded on samples with or without dilution in $BaSO_4$ using a Harrick praying mantis diffuse reflectance accessory mounted in a Perkin Elmer Lambda 650 UV–Vis spectrophotometer. The photo catalyst powder was well ground with of $BaSO_4$ and spread onto the sampling plate prior to the measurement. The background reflectance of $BaSO_4$ (reference) was measured before. The Kubelka-Munk function $F(R_\infty)$ was calculated as $F(R_\infty) = (1- R_\infty)^2/2R_\infty$, where R_∞ is diffuse reflectance of the sample relative to the reflectance of a standard according to the Kubelka-Munk theory.

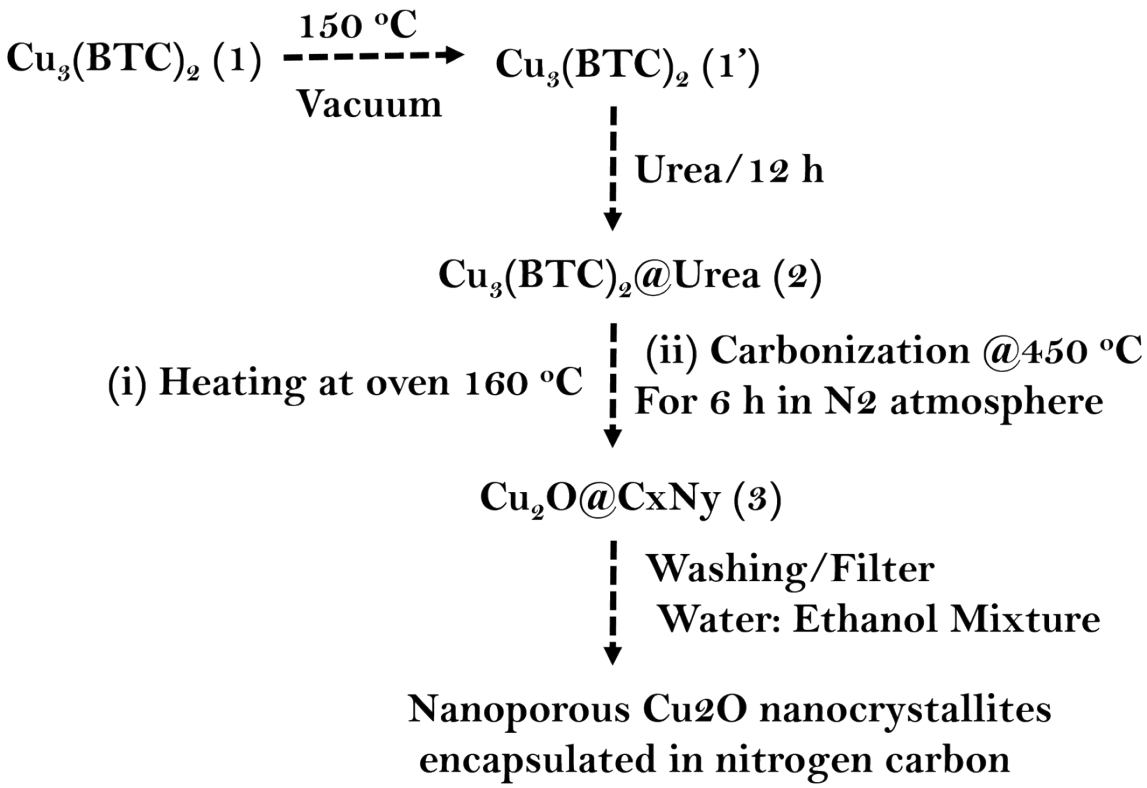

Scheme S1. Flow chart, detailed synthetic methodology of composite Cu_2O nanoparticles anchored on graphitic nitrogen-rich carbon matrix.

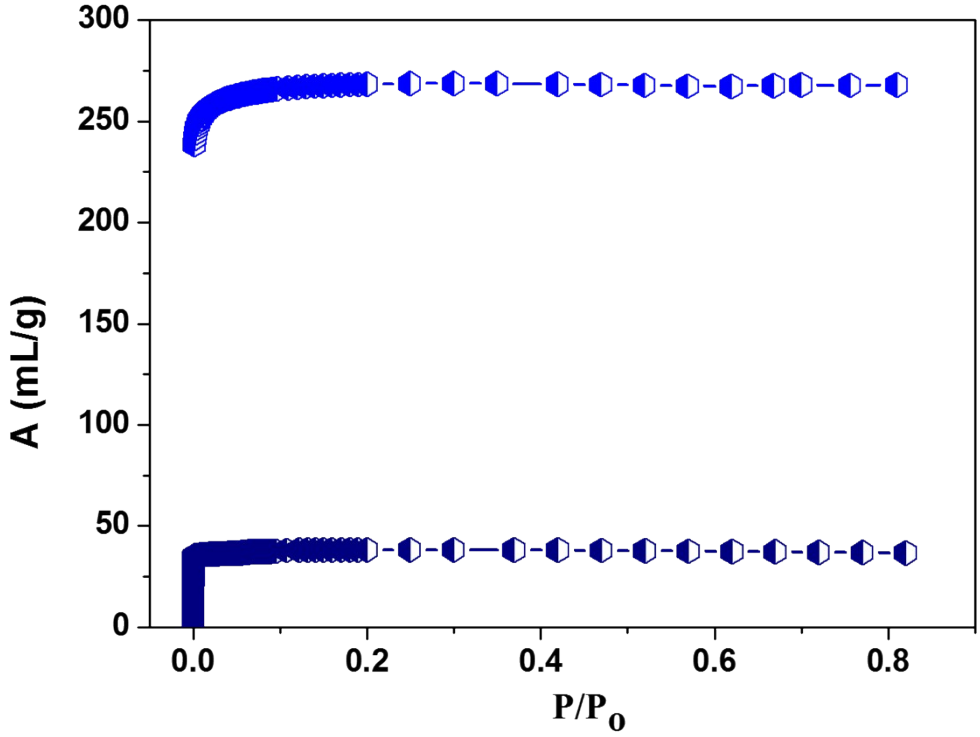

Fig S1. Nitrogen adsorption isotherms at 77 K of [Cu_3 $(BTC)_2$] and [$Cu_3(BTC)_2$@**Urea**]

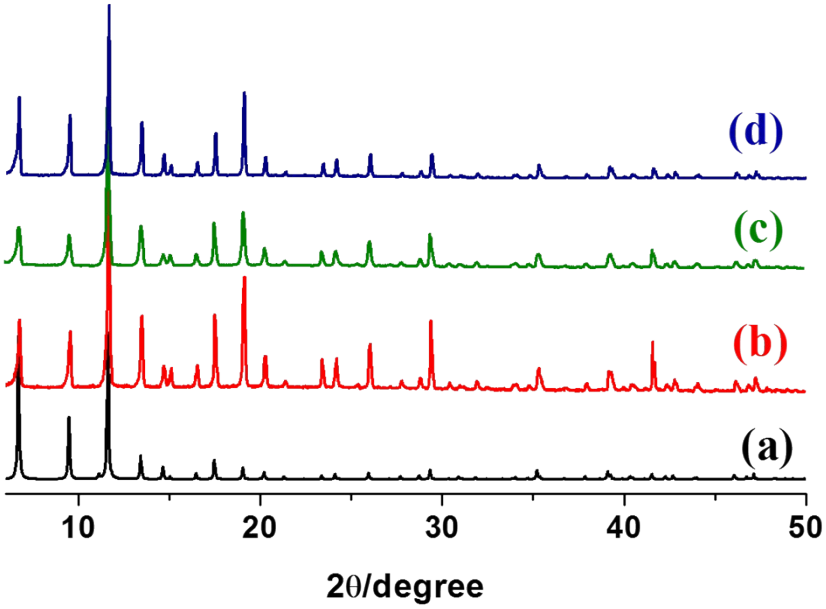

Fig S2. Powder XRD patterns of (a) simulated pattern [$Cu_3(BTC)_2$](**1**) (b) assynthesized [$Cu_3(BTC)_2$](**1**) (c) desolvated[$Cu_3(BTC)_2$](**1'**) (d) [$Cu_3(BTC)_2$@Urea](**2**) and it reveals structural integrity after inclusion of urea molecules on desolvated MOF.

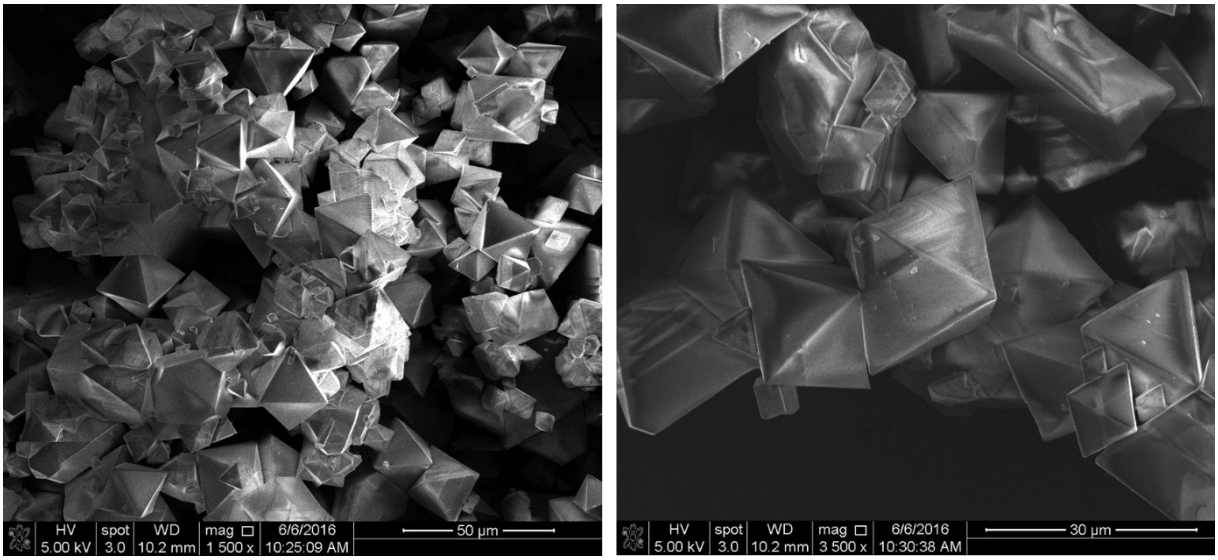

Fig S3. SEM images of **[$Cu_3(BTC)_2$]** showing octahedron morphology crystals

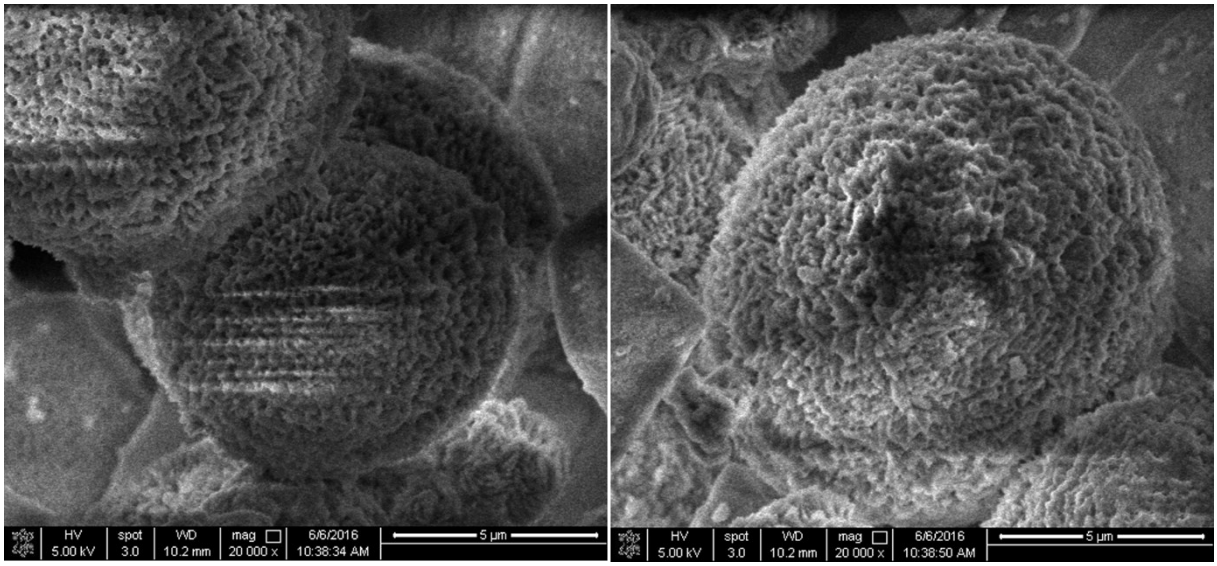

Fig S4. SEM images of [**$Cu_3(BTC)_2$@Urea**] composite reveals bundle of micron spheres.

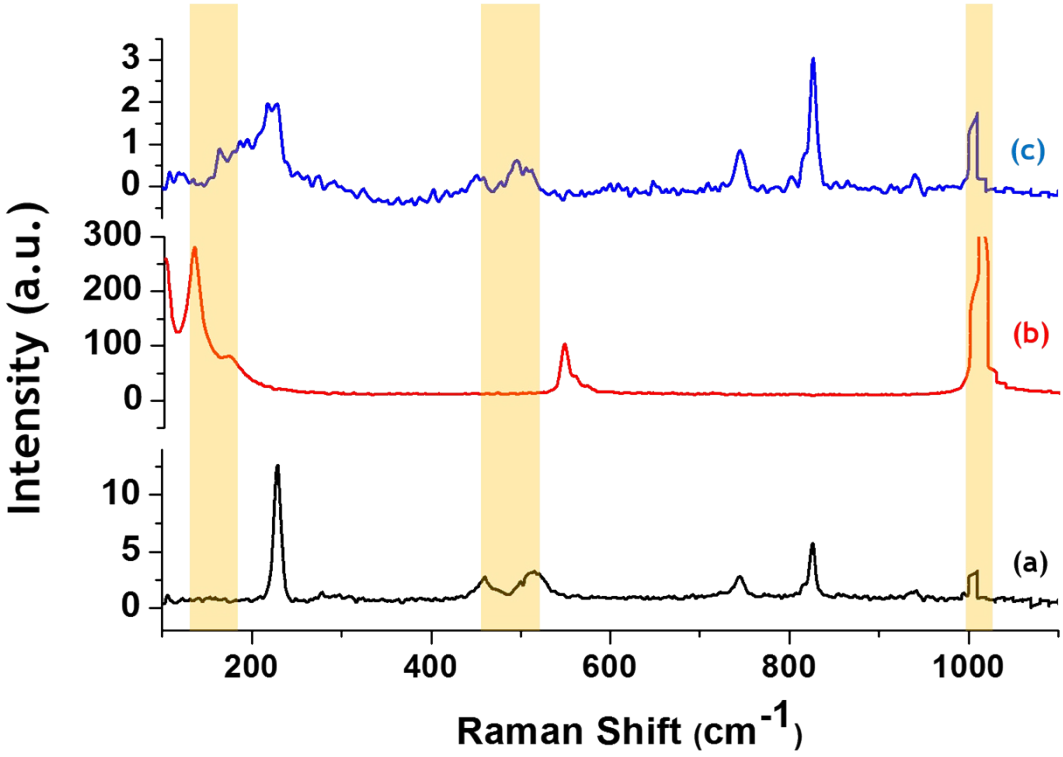

Fig S5. RAMAN spectrum (a) desolvated $[Cu_3(BTC)_2]$(**1'**) (b) Urea (c) hybrid $[Cu_3(BTC)_2$@Urea] reveals an additional band at 459 cm-1 corresponding to Cu-N band.

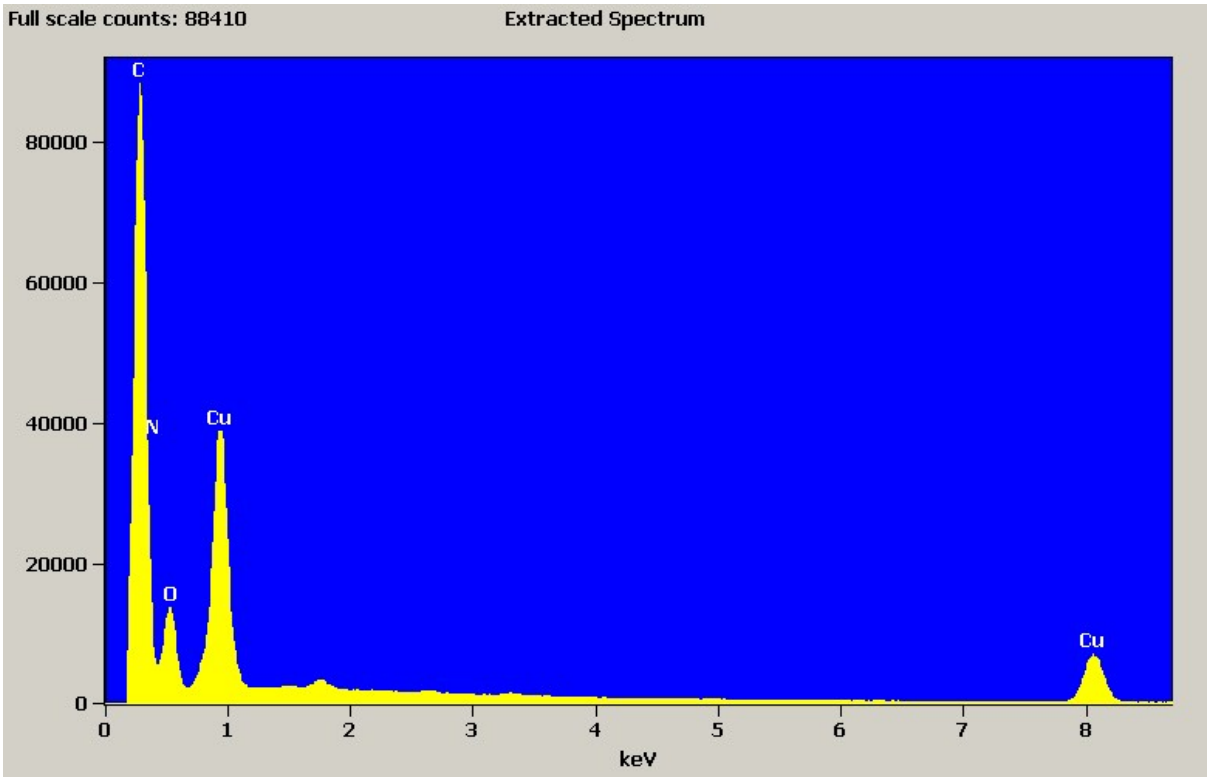

Fig S6a. The EDS spectra of resultant **Cu_2O@C_3N** composite, showing presence of Cu, C, N and O.

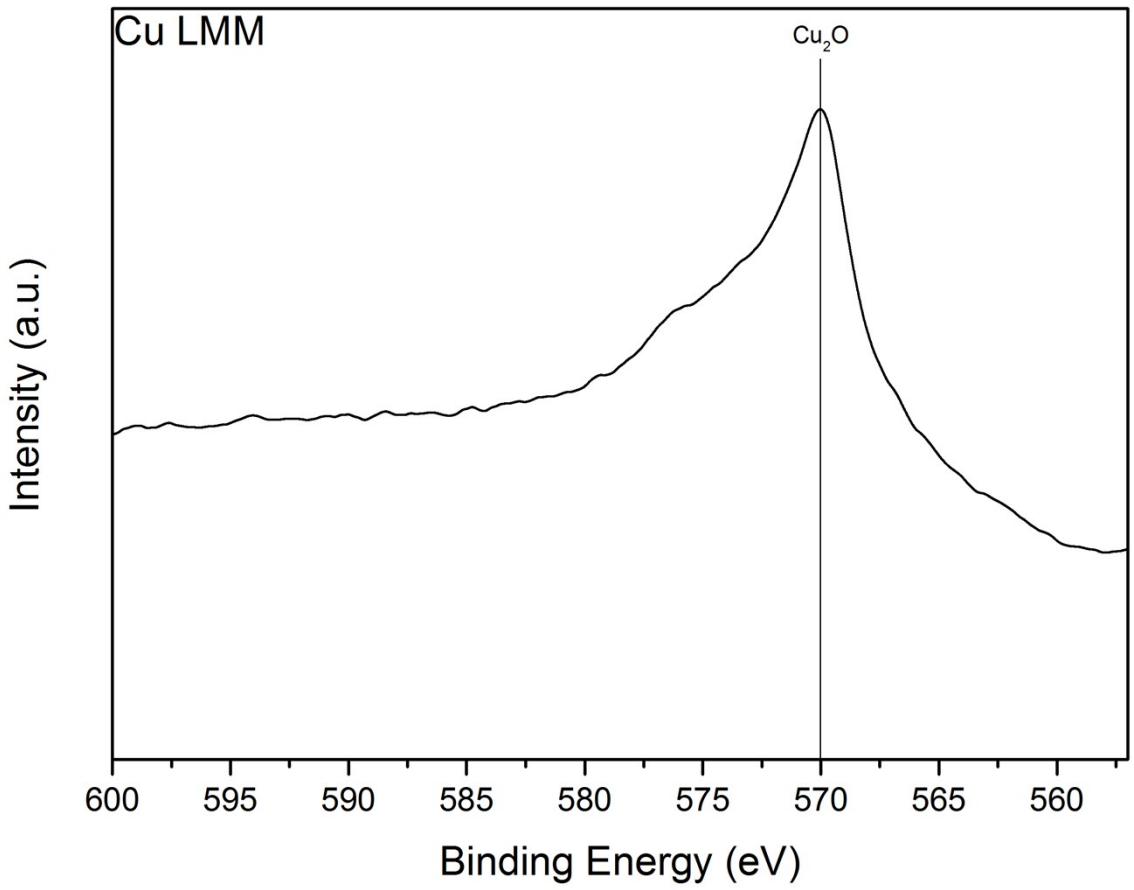

Fig S6b.Cu LMM Auger spectrum of resultant composite.

Cu is expected at the binding energy around 567.8 eV, while Cu_2O is located at 570.0 eV. The position and shape of the Cu LMM auger spectrum clearly proves the presence of Cu_2O. As referee suggested, this figure we provided in supporting information of revised manuscript.

References:

(1) Thomas Waechtler et al., Copper Oxide Films Grown by Atomic Layer Deposition from Bis(tri-n-butylphosphane)copper(I)acetylacetonate on Ta, TaN, Ru, and SiO_2, *J. Electrochem.* Soc. 2009, volume 156, issue 6, H453-H459

(2) Cu LMM spectra from http://www.xpsfitting.com/search/label/Copper (M.C. Biesinger, unpublished data (2013))

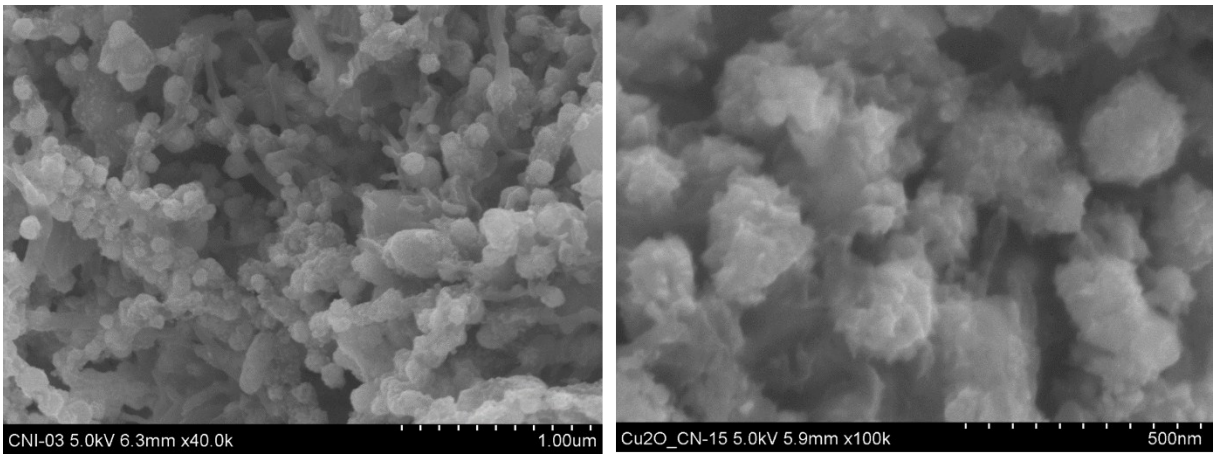

Fig S7a. FE-SEM image of **$Cu_2O@C_3N$** composite, showing presence of bundle of nano sheets

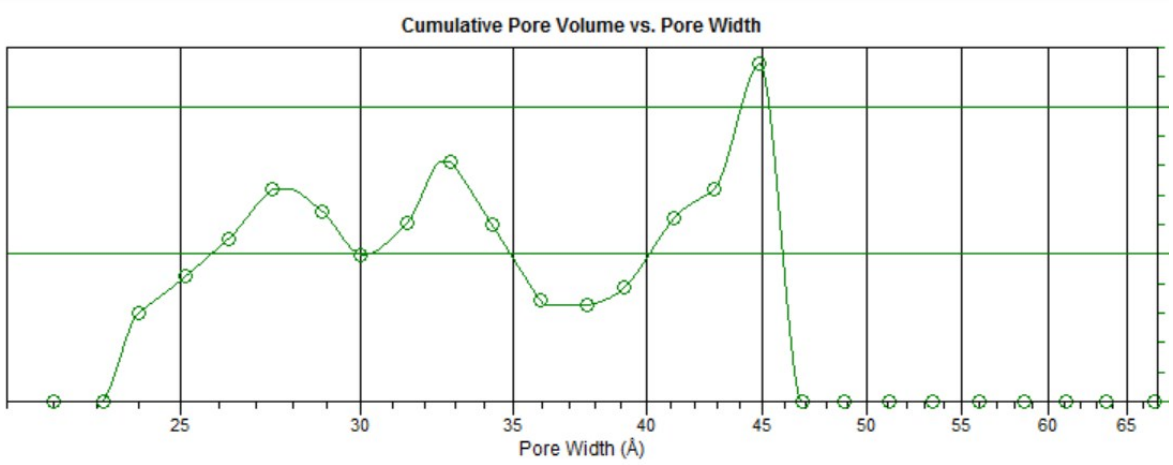

Fig. 7b. enlarged pore size distribution calculated from NLDFT method of $Cu_2O@C_3N$

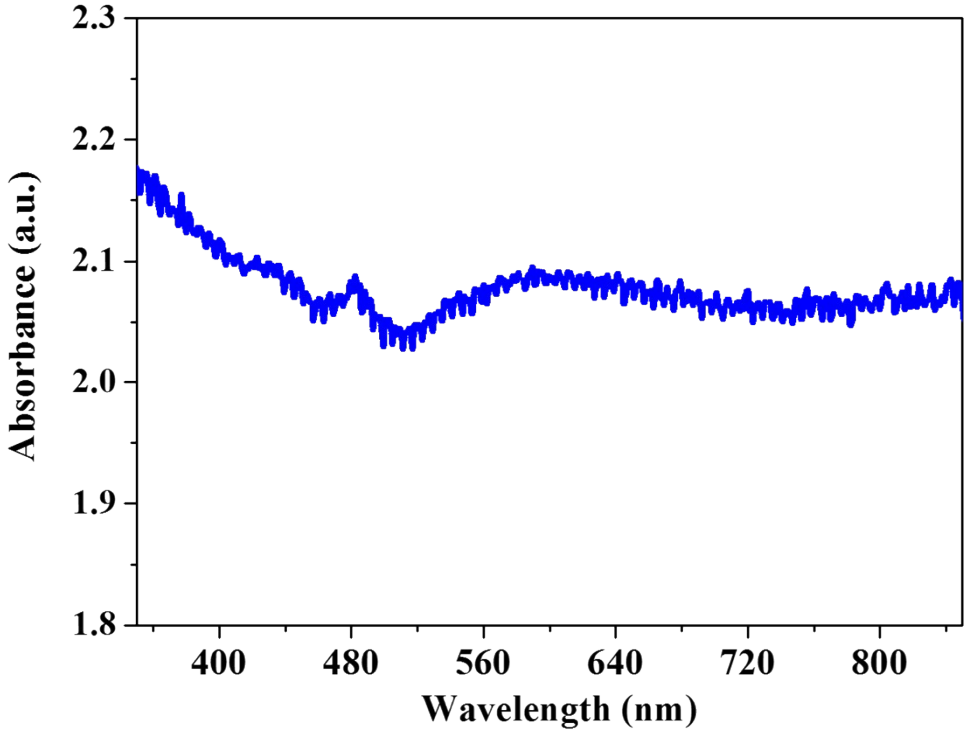

Fig S8. Uv-Vis diffuse spectra of **Cu_2O@C_3N** (band at 480 due instrumental error).

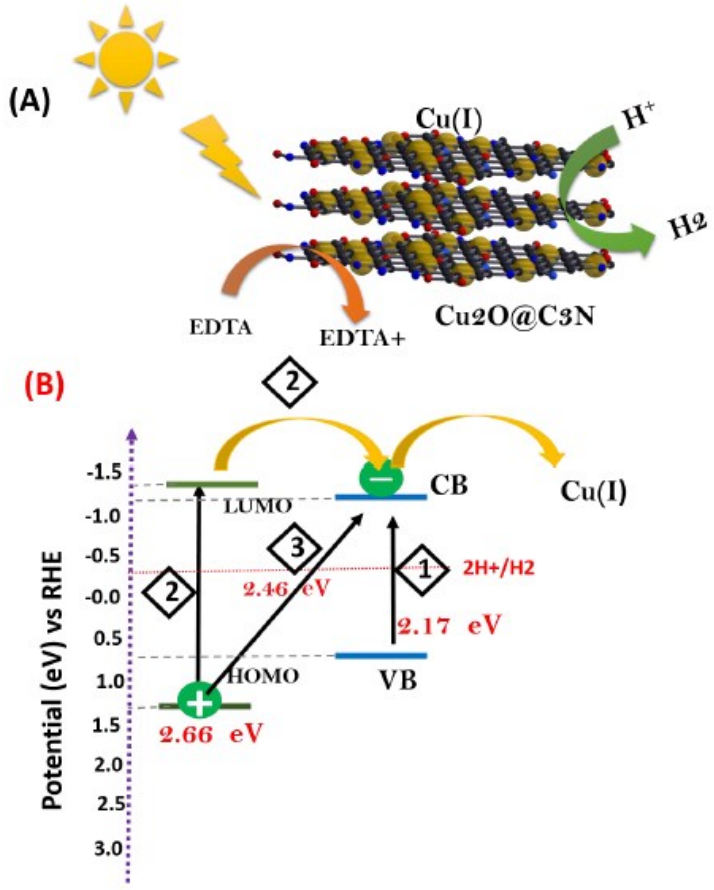

Fig.S9 (A) Schematic illustration of photocatalytic hydrogen production $Cu_2O@C_3N$ (cuprous oxide nanoparticle with nitrogen rich carbon matrix) in water under visible light irradiation, where EDTA as sacrificial donor. (B) Irradiation of CNx-Cu2O can result in photo indeced electron transfer by three distinct pathways, (i) Cu_2O bandgap excitation; (ii) excitation of CN_x ($HOMO_{CNx}$–$LUMO_{CNx}$), followed by electron transfer from $LUMO_{CNx}$ into the conduction band of Cu_2O (CB_{Cu2O}). (iii) Charge transfer excitation with direct optical electron transfer from $HOMO_{CNx}$ to CB_{Cu2O}. The CB_{Cu2O} electrons generated through pathways 1 to 3 are then transferred *via* copper centres of Cu_2O

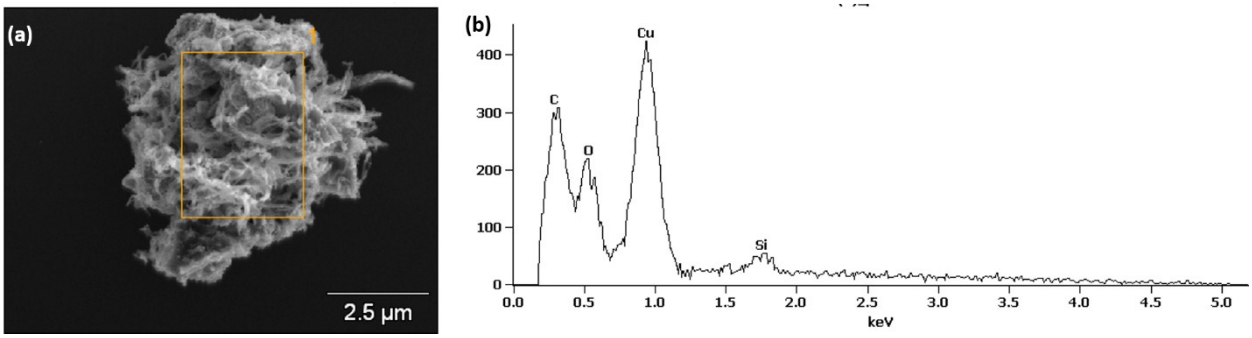

Fig S10. EDX spectra of carbonized sample **2**, carbonized at 550 ^{o}C

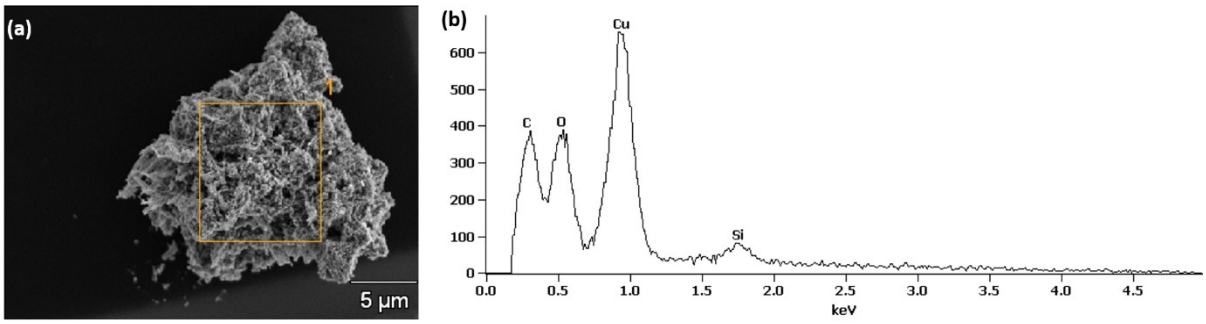

Fig S11. EDX spectra of carbonized sample **2**, carbonized at 700 ^{o}C

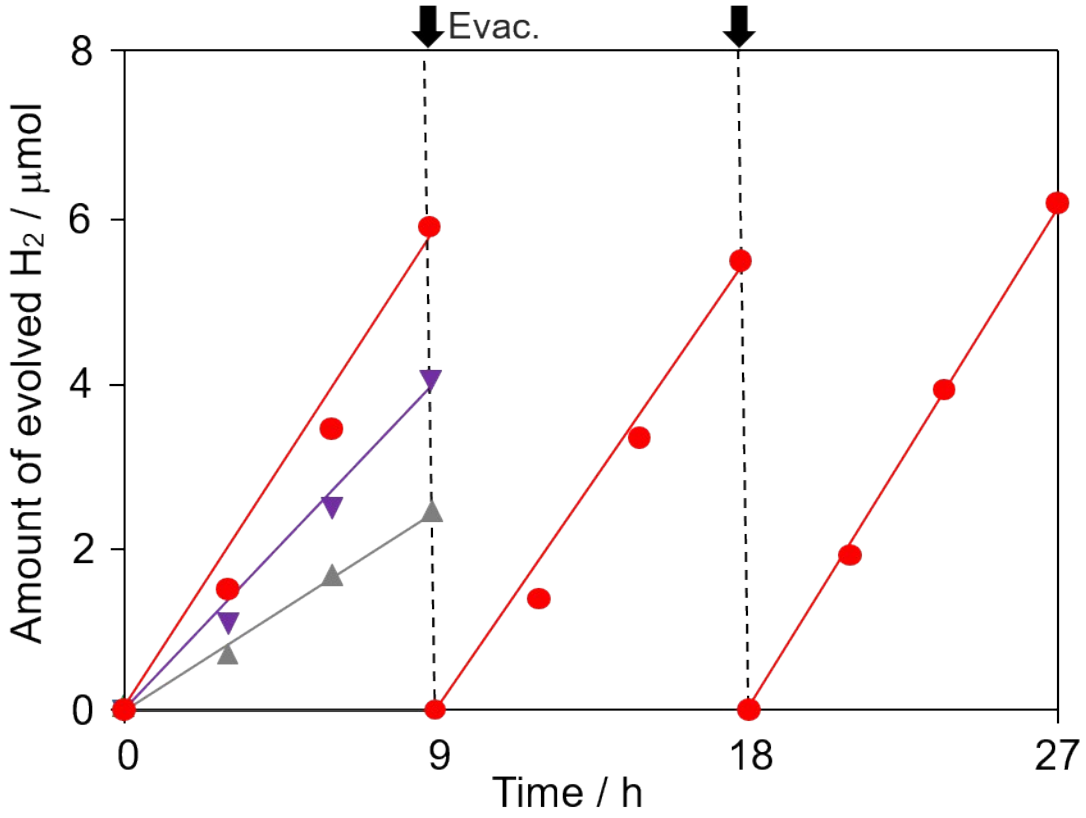

Fig S12. Comparison of photocatalytic H_2 Production of pyrolised composite [$Cu_3(BTC)_2$@Urea] at different temperatures 450 (red line), 550 (violet line),750 ^oC (grey line).

Table S1. Phocatalytic Activity of carbon nitride, Cuprous oxide and its composites for hydrogen production

S.No or Reference	Sample	CoCatalyst	Sacrificial Agent	Light Source	Hydrogen production (unit)	Reference photo catalyst	Enhancement and stability
1	g-C_3N_4 by urea polymerization	Phenyl urea	TEOA Triethanolamine	300 W Xe lamp (λ > 420 nm)	535 μmol h^{-1}	Pure g-C_3N_4	9 times ~16h
2	$Cu(OH)_2$/g-C_3N_4	$Cu(OH)_2$	methanol and water	300 W Xe lamp (λ > 400 nm)	48.7 μmol g^{-1} h^{-1}	Cu/g-C_3N_4	**1.92 times** >28 h
3	UiO-66/g-C_3N_4/P	UiO-66 Pt	Ascorbic acid	300 W Xe lamp (λ > 420 nm)	14.11x10 $^{-6}$ M h^{-1}	g-C_3N_4	NA
4	Au/g-C_3N_4		TEOA	500 W HBO lamp (λ > 420 nm)	10.70 μmol h^{-1}	Pt/g-C_3N_4	**4.65** >15 h
5	$Ni(OH)_2$/g-C_3N_4	$Ni(OH)_2$	TEOA	350 W Xe lamp with a 400 nm	7.60 μmol h^{-1}	Pure g-C_3N_4	**1.1** >12 h
6	Ni/NiO/g-C_3N_4	Ni/NiO	TEOA	300 W Xe lamp with a 420 nm	10 μmol h^{-1}	Pure g-C_3N_4	**10** >16 h
7	Ag_2O/g-C_3N_4	Ag_2O	TEOA	300 W Xe lamp with a 420 nm	32.88 μmol g^{-1} h^{-1}	g-C_3N_4	**274** >8 h
8	C, N-TiO_2/g-C_3N_4	C, N-TiO_2	TEOA	300 W Xe lamp with a 400 nm	39.18 μmol g^{-1} h^{-1}	C, N-TiO_2	10.9 >32 h
9	Cu_2O/rGO	Pt/Cu2O	Methanol/H2O	150W Xe lamp with 400 nm	264.5 μmol H_2 h^{-1}	Cu_2O	**3.5** NA
10	Cu_2O@g-C_3N_4	-Pt	TEOA	300 W Xe lamp with a 420 nm	243.0 μmol/h/g	pure g-C_3N_4	**1.72** NA
11	Cu_2O/rGO	-	TEOA	300 W Xe lamp with a 420 nm	4.53 mmol/h/g	rGO	**7.3**
12 Present work	Cu_2O@C3N	-	EDTA	500 W Xe lamp with a 420 nm	17.6 μmol/g For 27 h	Pure Cu_2O	**4** 27h

1. G.Zhang, X.A. Wang, J. Catal. 2013, 307, 246-253.
2. X.Zhou, Z.Luo, P. Tao, B.Jin, Z.Wu, Y. Huang, Mater. Chem. Phys. 2014, 143, 1462– 1468.
3. R.Wang, L. Gu, J.Zhou, X. Liu, F. Teng, C. Li, Y.Shen, Y. Yuan Adv. Mater. Interfaces 2015, 2, 1500037.
4. Y.Di, X.Wang, A. Thomas, M. Antonietti, ChemCatChem 2010, 2, 834– 838.
5. J.Yu, S.Wang, B. Cheng, Z.Lin, F. Huang, Catal. Sci. Technol. 2013, 3, 1782– 1789.
6. G. Zhang, G. Li, X. Wang, ChemCatChem 2015, 7, 2864– 2870.
7. M. Wu, J.M. Yan, X. W.Zhang, M. Zhao, Q. Jiang, J. Mater. Chem. A 2015, 3, 15710– 15714
8. W.Chen, T.Y. Liu, T. Huang, X.H. Liu, G. R. Duan, X. J. Yang, M. S. Chen, RSC Adv. 2015, 5, 101214–101220,
9. P. D. Tran, S. K. Batabyal, S. S. Pramana, J. Barber, L. H. Wong and S. C. J. Loo, Nanoscale, 2012, 4, 3875–3878.
10. X. Chen, S. Shen, L. Guo and S. S. Mao, Chem. Rev., 2010, 110, 6503.
11. H. Li, X. Li, S. Kang, L. Qin, G. Li, J. Mu, Int. J. Hydrogen Energy. 2014, 24, 11578-11582.

Table S2. The carbonization of **2** at various temperatures and corresponding oxidation state and nitrogen amount.

Sample	Copper phase	Nitrogen Content (%)
$[Cu_3(BTC)2@Urea]$ -450	Cu_2O (cuprous oxide)	14
$[Cu_3(BTC)2@Urea]$ -550	CuO (copper oxide)	0
$[Cu_3(BTC)2@Urea]$ -700	Cu (copper metal)	0

Table S3. Photocatalytic Hydrogen production at different time intervals.

Sample	Reaction time (h)	Total amount of H_2 evolved(μmol)
$Cu_2O@C_3N$	3	1.6
	6	3.5
	9	5.9
$Cu_2O@C_3N$_2nd cycle	3	1.4
	6	3.3
	9	5.5
$Cu_2O@C_3N$ _3rd cycle	3	1.9
	6	3.8
	9	6.2
Carbon nitride	9	2.8
Cuprous oxide	9	1.6
$Cu_3(BTC)_2$@Urea _550	3	1.2
	6	2.6
	9	4.1
$Cu_3(BTC)_2$@Urea _700	3	0.7
	6	1.7
	9	2.5